APPENDIX A—MXER SIMULATION STUDY, PART I

STAR, Inc.

MXER SIMULATION STUDY

E. M. LEVIN

Part I

Prepared for MSFC
November 17, 2005

Typeset by $\mathcal{A}\mathcal{M}\mathcal{S}$-TEX

NOMENCLATURE

A = first end-body
B = second end-body
C = center of mass of the tether system
E = longitudinal stiffness of the tether
J_C = moment of inertia of the tether system
L = total tether length
L_k = length of the k-th segment of the tether
m_A = mass of the first end-body
m_B = mass of the second end-body
m_k = embedded mass k
R = geocentric radius
R_E = mean radius of the Earth
R_C = geocentric radius of the center of mass
s = arclength along the unstretched tether
T = tether tension
t = time
γ = tether elongation
ρ = tether mass per unit length
λ = longitude
τ = unit vector along the tether line
τ_1 = direction of the imaginary straight tether line
Ω = rotational angular rate
$(\dot{\ })$ = differentiation with respect to time
$(\ ')$ = differentiation with respect to the arclength

1. FORMULATION OF THE PROBLEM

In this study, we consider the dynamics of a spinning tether system in an elliptical orbit in application to the Momentum Exchange Electrodynamic Reboost system. Momentum exchange tether systems have been studied in a variety of applications since Hans Moravec's early publication [1]. It has recently been suggested that momentum exchange systems can be enhanced with electrodynamic reboost between payload transfers [2-4].

The Momentum Exchange Electrodynamic Reboost system (MXER) has a projected tether span of up to 100 km, and spins rapidly with a period of 6-7 min. It is placed in an orbit with a low perigee of about 400 km and a high apogee of about 8000 km. To capture a payload at a perigee rendezvous, within a window of a few seconds, the motion of the system has to be predicted with very high precision, having acceptable position errors on the order of 1 m.

While this level of precision is routinely achieved today for conventional (non-tethered) satellites, it is much more difficult to achieve for a 100 km long flexible tether system. It is the goal of this study to investigate theoretical aspects of the dynamics and offer a practical approach to high precision dynamic modeling of a typical momentum exchange tether system.

2. DYNAMIC MODEL AND EQUATIONS OF MOTION

For the purposes of this study, we will assume that the momentum exchange system consists of two end-bodies A and B, modeled as point masses m_A and m_B, respectively, and a number of embedded masses m_k, $k = 1, \ldots, K$, connected with tether segments of lengths L_k, as shown in Fig. 1. Mass m_A can be counted as m_0, and mass m_B as m_{K+1}. Segment L_k connects masses m_k and m_{k+1}.

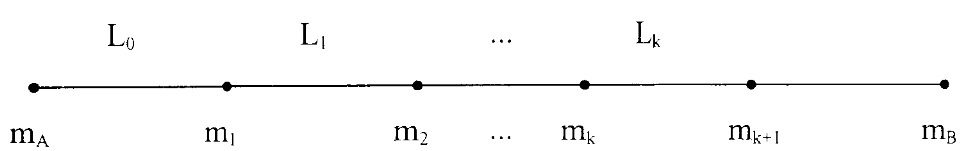

Fig. 1. Structure of the momentum exchange tether system.

All point masses and the masses of the tether segments are assumed to be constant. Tether mass per unit length can vary along the tether.

Positions of the tether elements with respect to a non-rotating geocentric reference frame $OXYZ$ are defined by the geocentric radius $\mathbf{R}$ as a function of the arclength s measured along the unstreched tether from A to B, and time t,

$$\mathbf{R} = \mathbf{R}(s,t),$$

Positions of the end masses and embedded masses are

$$\mathbf{R}_A = \mathbf{R}(s_A,t), \quad \mathbf{R}_B = \mathbf{R}(s_B,t), \quad \mathbf{R}_k = \mathbf{R}(s_k,t).$$

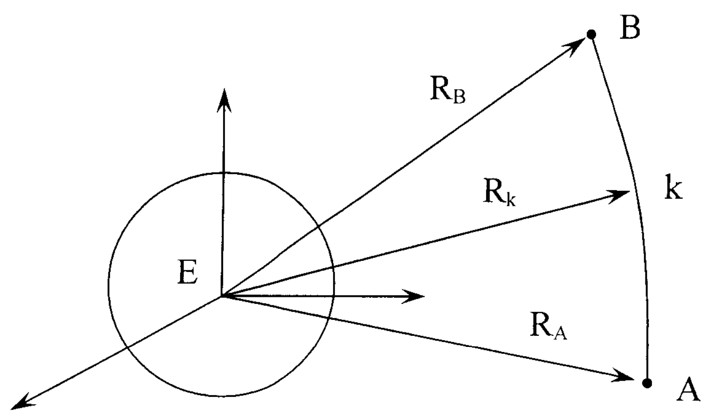

Fig. 2. Positions of the tether system elements.

The tension vector of a perfectly flexible tether is tangent to the tether line

$$\mathbf{T} = \frac{T}{\gamma}\mathbf{R}', \qquad \gamma = |\mathbf{R}'|. \tag{1}$$

where prime denotes differentiation with respect to the arclength s, and γ is the local tether elongation.

The tether tension can be expressed as a function of the elongation γ, elongation rate $\dot{\gamma}$, temperature Θ, and other factors, such as creep history,

$$T = T(s,\, t,\, \gamma,\, \dot{\gamma},\, \Theta, \ldots). \tag{2}$$

Equations of motion of the tether system constitute a mix of ordinary and partial differential equations [5]. The motion of the end masses and embedded masses is described by the ordinary differential equations

$$
\begin{aligned}
m_A \ddot{\mathbf{R}}_A &= \mathbf{T}_A + m_A \mathbf{g}_A + \mathbf{F}_A \\
m_B \ddot{\mathbf{R}}_B &= -\mathbf{T}_B + m_B \mathbf{g}_B + \mathbf{F}_B \\
m_k \ddot{\mathbf{R}}_k &= \mathbf{T}_{k+} - \mathbf{T}_{k-} + m_k \mathbf{g}_k + \mathbf{F}_k
\end{aligned}
\tag{3}
$$

where dots denote differentiation with respect to time, $\mathbf{g}_A$, $\mathbf{g}_B$, and $\mathbf{g}_k$ are the gravity accelerations at points A, B, and k, respectively, $\mathbf{F}_A$, $\mathbf{F}_B$, and $\mathbf{F}_k$ are non-gravitational forces acting on the end masses and embedded masses. The tether tension vectors are taken at the following points: $\mathbf{T}_A$ at point A, $\mathbf{T}_B$ at point B, $\mathbf{T}_{k-}$ at point k of segment L_{k-1}, and $\mathbf{T}_{k+}$ at point k of segment L_k.

The motion of the tether is described by the partial differential equation

$$
\rho \ddot{\mathbf{R}} = \mathbf{T}' + \rho \mathbf{g} + \mathbf{F} \tag{4}
$$

where dots denote differentiation with respect to time t, and primes denote differentiation with respect to the arclength s, ρ is the tether mass per unit length, and $\mathbf{T}$ is the tether tension.

3. GRAVITATIONAL FIELD MODEL

The gravitational field is a sum of the gravitational field of the Earth and other celestial bodies, primarily, the Moon and the Sun.

The geopotential U is usually represented as

$$
U = \frac{\mu_E}{R} \sum_{n=0}^{\infty} \sum_{m=0}^{n} \left(\frac{R_E}{R}\right)^n (\bar{C}_{nm} \cos m\lambda + \bar{S}_{nm} \sin m\lambda)\, \bar{P}_{nm}(\cos\alpha), \tag{5}
$$

where μ_E is the gravitational constant of the Earth, R_E is the equatorial radius of the Earth, R is the geocentric radius, λ is the geographical longitude eastward from Greenwich, α is the geocentric colatitude (the angle between the rotation axis of the Earth and the geocentric radius of a point, $\alpha = 0$ at the North Pole), $\bar{P}_{nm}$ are normalized Legendre functions,

$$
\bar{P}_{nm}(\cos\alpha) = \varkappa_n^m P_n^m(\cos\alpha),
$$

$\varkappa_n^m$ is a norm,

$$\varkappa_n^0 = \sqrt{2n+1}, \qquad \text{with} \quad m = 0,$$

$$\varkappa_n^m = \sqrt{\frac{2\,(2n+1)\,(n-m)!}{(n+m)!}}, \qquad \text{with} \quad m > 0,$$

and P_n^m are associated Legendre functions of degree n and order m,

$$P_n^m(x) = (1-x^2)^{m/2}\,\frac{d^m}{dx^m}P_n(x), \qquad P_n(x) = \frac{1}{2^n n!}\frac{d^n}{dx^n}(x^2-1)^n,$$
$$P_0^0 = 1,$$
$$P_1^0(\cos\alpha) = \cos\alpha,$$
$$P_1^1(\cos\alpha) = \sin\alpha,$$
$$P_2^0(\cos\alpha) = \frac{1}{4}(3\cos 2\alpha + 1) = \frac{1}{2}(3\cos^2\alpha - 1),$$
$$P_2^1(\cos\alpha) = \frac{3}{2}\sin 2\alpha = 3\sin\alpha\cos\alpha,$$
$$P_2^2(\cos\alpha) = \frac{3}{2}(1-\cos 2\alpha) = 3\sin^2\alpha,$$
$$P_3^0(\cos\alpha) = \frac{1}{8}(5\cos 3\alpha + 3\cos\alpha) = \frac{1}{2}(5\cos^3\alpha - 3\cos\alpha),$$
$$P_3^1(\cos\alpha) = \frac{3}{8}(\sin\alpha + 5\sin 3\alpha) = \frac{3}{2}\sin\alpha(5\cos^2\alpha - 1),$$
$$P_3^2(\cos\alpha) = \frac{15}{4}(\cos\alpha - \cos 3\alpha) = 15\sin^2\alpha\cos\alpha,$$
$$P_3^3(\cos\alpha) = \frac{15}{4}(3\sin\alpha - \sin 3\alpha) = 15\sin^3\alpha,$$
$$\ldots$$

The components of the gravitational acceleration $\mathbf{g} = \nabla U$ are

$$g_R = \frac{\partial U}{\partial R}, \qquad g_\alpha = \frac{1}{R}\frac{\partial U}{\partial \alpha}, \qquad g_\lambda = \frac{1}{R\sin\alpha}\frac{\partial U}{\partial\lambda},$$

where g_R is pointing along the geocentric radius, g_α is pointing southward along the meridian, and g_λ is pointing eastward along the parallel. In the geocentric axes OXYZ,

$$g_x = (g_R\cos\varphi + g_\alpha\sin\varphi)\cos\lambda - g_\lambda\sin\lambda$$
$$g_y = (g_R\cos\varphi + g_\alpha\sin\varphi)\sin\lambda + g_\lambda\cos\lambda$$
$$g_z = g_R\sin\varphi - g_\alpha\cos\varphi$$

where $\varphi = \pi/2 - \alpha$ is the latitude.

To properly evaluate convergence, we should use a geopotential model of the maximum available degree and order. An obvious choice is the Earth Gravity Model EGM96 [6], of degree and order 360.

According to this model, $\mu_E = 398600.4415$ km^3/sec^2, $R_E = 6378.1363$ km, and the normalized coefficients $\bar{C}_{nm}$ and $\bar{S}_{nm}$ are as follows:

$\bar{C}_{0,0} = 1,$	$\bar{S}_{0,0}$ – not used
$\bar{C}_{1,0} = 0,$	$\bar{S}_{1,0}$ – not used
$\bar{C}_{1,1} = 0,$	$\bar{S}_{1,1} = 0,$
$\bar{C}_{2,0} = -0.484165371736 \cdot 10^{-3},$	$\bar{S}_{2,0}$ – not used
$\bar{C}_{2,1} = -0.186987635955 \cdot 10^{-9},$	$\bar{S}_{2,1} = 0.119528012031 \cdot 10^{-8},$
$\bar{C}_{2,2} = 0.243914352398 \cdot 10^{-5},$	$\bar{S}_{2,2} = -0.140016683654 \cdot 10^{-5},$
$\bar{C}_{3,0} = 0.957254173792 \cdot 10^{-6},$	$\bar{S}_{3,0}$ – not used
$\bar{C}_{3,1} = 0.202998882184 \cdot 10^{-5},$	$\bar{S}_{3,1} = 0.248513158716 \cdot 10^{-6},$
$\bar{C}_{3,2} = 0.904627768605 \cdot 10^{-6},$	$\bar{S}_{3,2} = -0.619025944205 \cdot 10^{-6},$
$\bar{C}_{3,3} = 0.721072657057 \cdot 10^{-6},$	$\bar{S}_{3,3} = 0.141435626958 \cdot 10^{-5},$
...	...
$\bar{C}_{360,359} = 0.183971631467 \cdot 10^{-10},$	$\bar{S}_{360,359} = -0.310123632209 \cdot 10^{-10},$
$\bar{C}_{360,360} = -0.447516389678 \cdot 10^{-24},$	$\bar{S}_{360,360} = -0.830224945525 \cdot 10^{-10}$

Gravitational perturbations caused by the Earth tides can be described by time dependent variations in the geopotential expansion coefficients [7].

Gravitational perturbations caused by a celestial body of mass M_p located at $\mathbf{R}_p$ with respect to the geocentric axes $OXYZ$ are described as

$$\mathbf{g}_p = GM_p \left(\frac{\mathbf{R}_p - \mathbf{R}}{|\mathbf{R}_p - \mathbf{R}|^3} - \frac{\mathbf{R}_p}{R_p^3} \right), \tag{6}$$

where G is the universal gravity constant, and $R_p = |\mathbf{R}_p|$.

For most practical purposes and for all celestial bodies, except the Moon, the linear approximation

$$\mathbf{g}_p = \frac{GM_p}{R_p^3} \left[3\mathbf{e}_p(\mathbf{e}_p, \mathbf{R}) - \mathbf{R} \right], \tag{7}$$

where $\mathbf{e}_p = \mathbf{R}_p / R_p$ is a unit vector of the direction to the celestial body, should be adequate [7].

4. STATIONARY ROTATION

If we disregard non-gravitational forces $\mathbf{F}$ in equations (3)–(4) and assume that the tether is inextensible ($\gamma = |\mathbf{R}'| = 1$) and gravitational acceleration does not vary along the tether ($\mathbf{g} = \mathbf{g}_C$), then equations (3)–(4) will have a stationary solution

$$\mathbf{T} = T(s)\,\boldsymbol{\tau}(t), \qquad \mathbf{R} = \mathbf{R}_C(t) + (s - s_C)\,\boldsymbol{\tau}(t), \tag{8}$$

where $\mathbf{R}_C(t)$ and $\boldsymbol{\tau}(t)$ are determined from

$$\ddot{\mathbf{R}}_C = \mathbf{g}_C, \qquad \ddot{\boldsymbol{\tau}} = -\Omega^2\,\boldsymbol{\tau}. \tag{9}$$

Here, $\mathbf{R}_C$ is the radius-vector of the center of mass, moving as a point mass, $\mathbf{g}_C$ is the gravity acceleration at the center of mass, $\boldsymbol{\tau}$ is a unit vector along the tether line rotating at a constant angular velocity $\boldsymbol{\Omega}$ in a fixed plane normal to $\boldsymbol{\Omega}$, $\Omega = |\boldsymbol{\Omega}|$, s_C is the arclength corresponding to the center of mass

$$s_C = \frac{1}{M}\left(m_A s_A + m_B s_B + \sum_k m_k s_k + \int_A^B \rho\, s\, ds\right), \tag{10}$$

and M is the total mass of the tether system.

In the stationary motion (8)–(9), we have

$$\ddot{\mathbf{R}} = \ddot{\mathbf{R}}_C + (s - s_C)\,\ddot{\boldsymbol{\tau}} = \mathbf{g}_C - (s - s_C)\,\Omega^2\boldsymbol{\tau}.$$

After substituting this relation into equations (3)–(4), we arrive at a boundary problem for the equilibrium tension,

$$\begin{aligned}
T' &= -\rho\,\Omega^2(s - s_C),\\
T_A &= -m_A\Omega^2(s_A - s_C),\\
T_B &= m_B\Omega^2(s_B - s_C),\\
T_{k+} &= T_{k-} - m_k\Omega^2(s_k - s_C),
\end{aligned} \tag{11}$$

where the last equation defines tension increments associated with the embedded masses m_k.

The equilibrium tension is obtained by solving the first equation of (11) with the initial condition $T = T_A$ given by the second equation and incrementing the tension at the points s_k, as described by the last equation of (11). The boundary

condition $T = T_B$ given by third equation is always satisfied because of the definition of the value s_C (10) and the structure of equations (11).

In general, the equilibrium tension increases from the value T_A at the end A to its maximum value T_C at the center of mass C, and then drops to the value T_B at the other end, as shown in Fig. 3.

To minimize mass, the tether should be tapered, with the linear density varying along the tether, $\rho = \rho(s)$. Ideally, the tether should be equally stressed/strained at all points,

$$\frac{T}{E} = \delta_*, \tag{12}$$

where E is the longitudinal tether stiffness, and δ_* is the maximum allowed strain. Condition (12) can be rewritten as

$$T = \rho\, v_E^2\, \delta_*, \qquad v_E = \sqrt{\frac{E}{\rho}}, \tag{13}$$

where v_E is the longitudinal wave velocity in the tether. Now, we can express the linear density as a function of tension, $\rho = T\, v_E^{-2}\, \delta_*^{-1}$, and substitute this relation into the first equation of the boundary problem (11) to produce a boundary problem for an ideal equally stressed/strained tether.

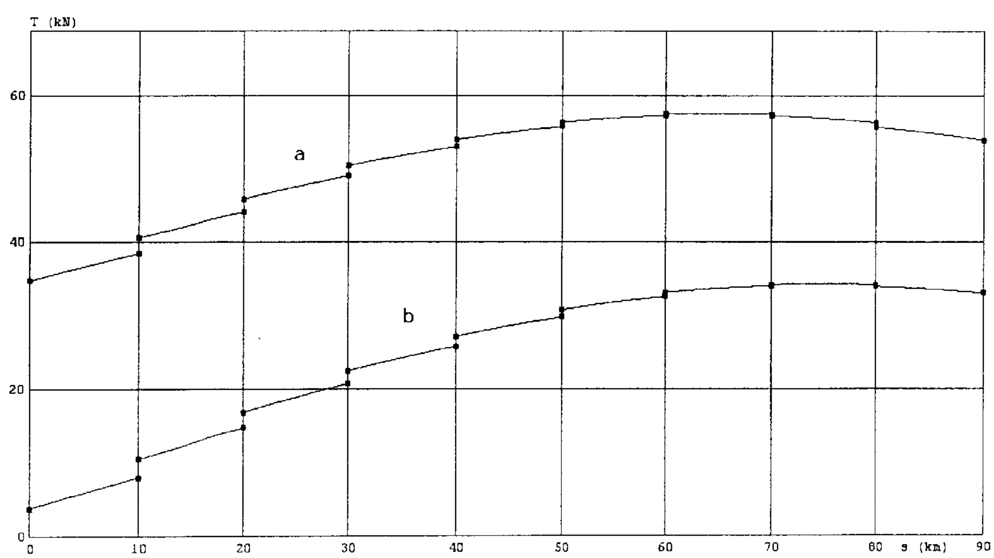

Fig. 3. Tension profile of a tether system with (a) and without (b) payload.

In practice, the tether can be made of a number of uniform segments, approximating the desired taper profile.

Typical tension profiles are shown in Fig. 3 for a 90 km tether system with $m_A = 250$ kg, $m_B = 11000$ kg, and 8 embedded masses $m_k = 200$ kg placed 10 km apart. The tethers are made of Zylon and are uniform on each segment with a maximum strain of $\delta_* = 0.01$. The system spins at $\Omega = 0.8$ deg/sec. In case (a), the end mass A carries a 2500 kg payload, and there is no payload in case (b).

5. SMALL OSCILLATIONS AND EIGENFORMS

To study small oscillations of the tether system about the stationary rotation, we introduce a rotating reference frame $C\xi\eta\zeta$, with the origin at the center of mass, axis $C\xi$ aligned with the tether line, and axis $C\zeta$ aligned with the angular rate vector $\mathbf{\Omega}$, so that

$$\boldsymbol{\tau} = (1,\, 0,\, 0), \qquad \mathbf{\Omega} = (0,\, 0,\, \Omega).$$

With respect to the rotating axes $C\xi\eta\zeta$, the stationary motion (8)–(9) is viewed as a relative equilibrium.

Equations of small oscillations of the tether system about the relative equilibrium are derived from (3)–(4),

$$\begin{aligned} \rho\, D(\delta\mathbf{r}) &= \delta\mathbf{T}', \\ m_A\, D(\delta\mathbf{r}_A) &= \delta\mathbf{T}_A, \\ m_B\, D(\delta\mathbf{r}_B) &= -\delta\mathbf{T}_B, \\ m_k\, D(\delta\mathbf{r}_k) &= \delta\mathbf{T}_{k+} - \delta\mathbf{T}_{k-}, \end{aligned} \tag{14}$$

where $\delta\mathbf{r}$ and $\delta\mathbf{T}$ are deviations from the relative equilibrium, and D denotes the linear expression

$$D(\delta\mathbf{r}) = \delta\ddot{\mathbf{r}} + 2\mathbf{\Omega}\times\delta\dot{\mathbf{r}} + \mathbf{\Omega}\times(\mathbf{\Omega}\times\delta\mathbf{r}),$$

in which derivatives are calculated with respect to the rotating axes $C\xi\eta\zeta$.

Small oscillations (14) have two independent components. One is normal to the tether line in the plane of the stationary rotation,

$$\delta\mathbf{r} = (0,\, \eta,\, 0), \qquad \delta\mathbf{T} = (0,\, T\eta',\, 0),$$

and the other one is normal to the rotation plane

$$\delta\mathbf{r} = (0,\, 0,\, \zeta), \qquad \delta\mathbf{T} = (0,\, 0,\, T\zeta').$$

There is no longitudinal component in the linear approximation for an inextensible tether.

Equations of small in-plane oscillations take the form

$$
\begin{aligned}
&\rho\,(\ddot{\eta} - \Omega^2 \eta) = (T\eta')', \\
&m_A\,(\ddot{\eta}_A - \Omega^2 \eta_A) = (T\eta')_A, \\
&m_B\,(\ddot{\eta}_B - \Omega^2 \eta_B) = -(T\eta')_B, \\
&m_k\,(\ddot{\eta}_k - \Omega^2 \eta_k) = (T\eta')_{k+} - (T\eta')_{k-},
\end{aligned}
\tag{15}
$$

After substituting $\eta = U_n(s)\,cos(\Omega_n t)$ into (15), we arrive at the following eigen-value problem,

$$
\begin{aligned}
&(TU_n')' = -\rho\,(\Omega_n^2 + \Omega^2)\,U_n, \\
&(TU_n')_A = -m_A\,(\Omega_n^2 + \Omega^2)\,U_{nA}, \\
&(TU_n')_B = m_B\,(\Omega_n^2 + \Omega^2)\,U_{nB}, \\
&(TU_n')_{k+} = (TU_n')_{k-} - m_k\,(\Omega_n^2 + \Omega^2)\,U_{nk},
\end{aligned}
\tag{16}
$$

Small out-of-plane oscillations are described by

$$
\begin{aligned}
&\rho\,\ddot{\zeta} = (T\zeta')', \\
&m_A\,\ddot{\zeta}_A = (T\zeta')_A, \\
&m_B\,\ddot{\zeta}_B = -(T\zeta')_B, \\
&m_k\,\ddot{\zeta}_k = (T\zeta')_{k+} - (T\zeta')_{k-}.
\end{aligned}
\tag{17}
$$

After substituting $\zeta = U_n(s)\,cos(\Omega_n t)$ into (17), we derive the following eigenvalue problem,

$$
\begin{aligned}
&(TU_n')' = -\rho\,\Omega_n^2\,U_n, \\
&(TU_n')_A = -m_A\,\Omega_n^2\,U_{nA}, \\
&(TU_n')_B = m_B\,\Omega_n^2\,U_{nB}, \\
&(TU_n')_{k+} = (TU_n')_{k-} - m_k\,\Omega_n^2\,U_{nk}.
\end{aligned}
\tag{18}
$$

The eigenvalue problems (16) and (18) are very similar. They have the same eigenfunctions $U_n(s)$, and their eigenfrequencies are bound by a simple relation,

$$
\Omega_{n\zeta}^2 = \Omega_{n\eta}^2 + \Omega^2. \tag{19}
$$

Analyzing the boundary problem (11) for the equilibrium tension and the eigenvalue problems (16), (18), we note that the eigenforms do not depend on the angular rate Ω. Indeed, we can introduce a normalized equilibrium tension

$$
P(s) = \frac{T(s)}{\Omega^2}, \tag{20}
$$

and rewrite equations (11) as

$$
\begin{aligned}
P' &= -\rho\,(s - s_C),\\
P_A &= -m_A(s_A - s_C),\\
P_B &= m_B(s_B - s_C),\\
P_{k+} &= P_{k-} - m_k(s_k - s_C),
\end{aligned}
\tag{21}
$$

while equations (16) and (18) can be reduced to

$$
\begin{aligned}
(PU_n')' &= -\rho\,\beta_n^2\,U_n,\\
(PU_n')_A &= -m_A\,\beta_n^2\,U_{nA},\\
(PU_n')_B &= m_B\,\beta_n^2\,U_{nB},\\
(PU_n')_{k+} &= (PU_n')_{k-} - m_k\,\beta_n^2\,U_{nk},
\end{aligned}
\tag{22}
$$

where β_n are dimensionless eigenvalues. The resulting system of equations (21)–(22) and its solutions do not depend on the angular rate Ω.

The eigenfrequencies $\Omega_{n\eta}$ and $\Omega_{n\zeta}$ can be expressed through the dimensionless eigenvalues β_n as

$$
\Omega_{n\eta} = \sqrt{\beta_n^2 - 1}\,\Omega, \qquad \Omega_{n\zeta} = \beta_n\Omega. \tag{23}
$$

The eigenvalue problem (21)–(22) has two trivial solutions,

$$
\beta_0 = 0, \qquad U_0 = 1, \tag{24}
$$

and

$$
\beta_1 = 1, \qquad U_1 = s - s_C. \tag{25}
$$

The first solution simply reduces the right and the left parts of (22) to zero, while the second solution reduces (22) to (21). Dynamically, solution (24) corresponds to perturbations of the motion of the center of mass, while solution (25) corresponds to variations of the angular rate and direction of the axis of the stationary rotation.

The trivial solutions are followed by an infinite series of solutions $\{\beta_n,\, U_n\}$, $n = 2, 3, \ldots$, which constitute an orthogonal basis with the orthogonality condition

$$
\langle U_i,\, U_j\rangle = 0, \qquad i \neq j, \tag{26}
$$

where

$$
\langle U_i,\, U_j\rangle = m_A(U_iU_j)_A + m_B(U_iU_j)_B + \sum_k m_k(U_iU_j)_k + \int_A^B \rho\,(U_iU_j)\,ds. \tag{27}
$$

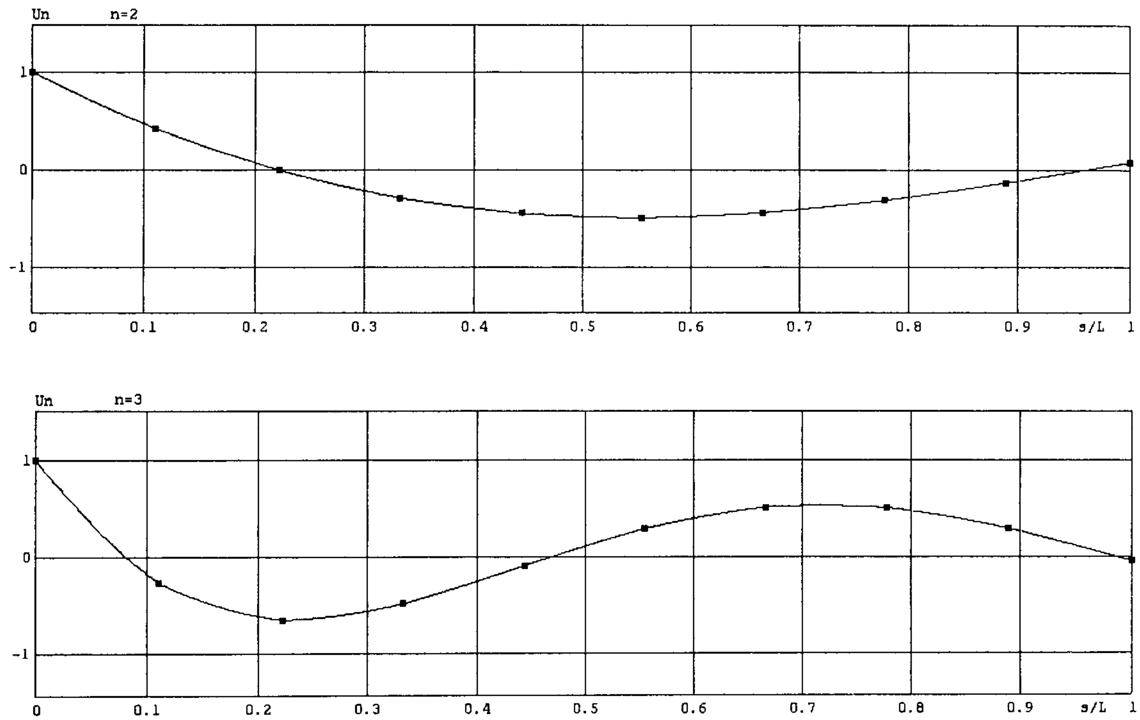

Fig. 4. Lower eigenforms of a spinning tether system ($n = 2, 3$).

The orthogonality condition can also be expressed as

$$\int_A^B P\, U_i' U_j'\, ds = 0, \qquad i \neq j. \tag{28}$$

The norms of the eigenfunctions are defined as

$$||U_n|| = \langle U_n,\, U_n \rangle. \tag{29}$$

The norm of the first trivial eigenfunction (24) is equal to the total mass of the tether system

$$||U_0|| = M = m_A + m_B + \sum_k m_k + \int_A^B \rho\, ds, \tag{30}$$

while the norm of the second trivial eigenfunction (25) is equal to the moment of inertia about the center of mass,

$$||U_1|| = J_C =$$
$$m_A\,(s_A - s_C)^2 + m_B\,(s_B - s_C)^2 + \sum_k m_k\,(s_k - s_C)^2 + \int_A^B \rho\,(s - s_C)^2 ds. \tag{31}$$

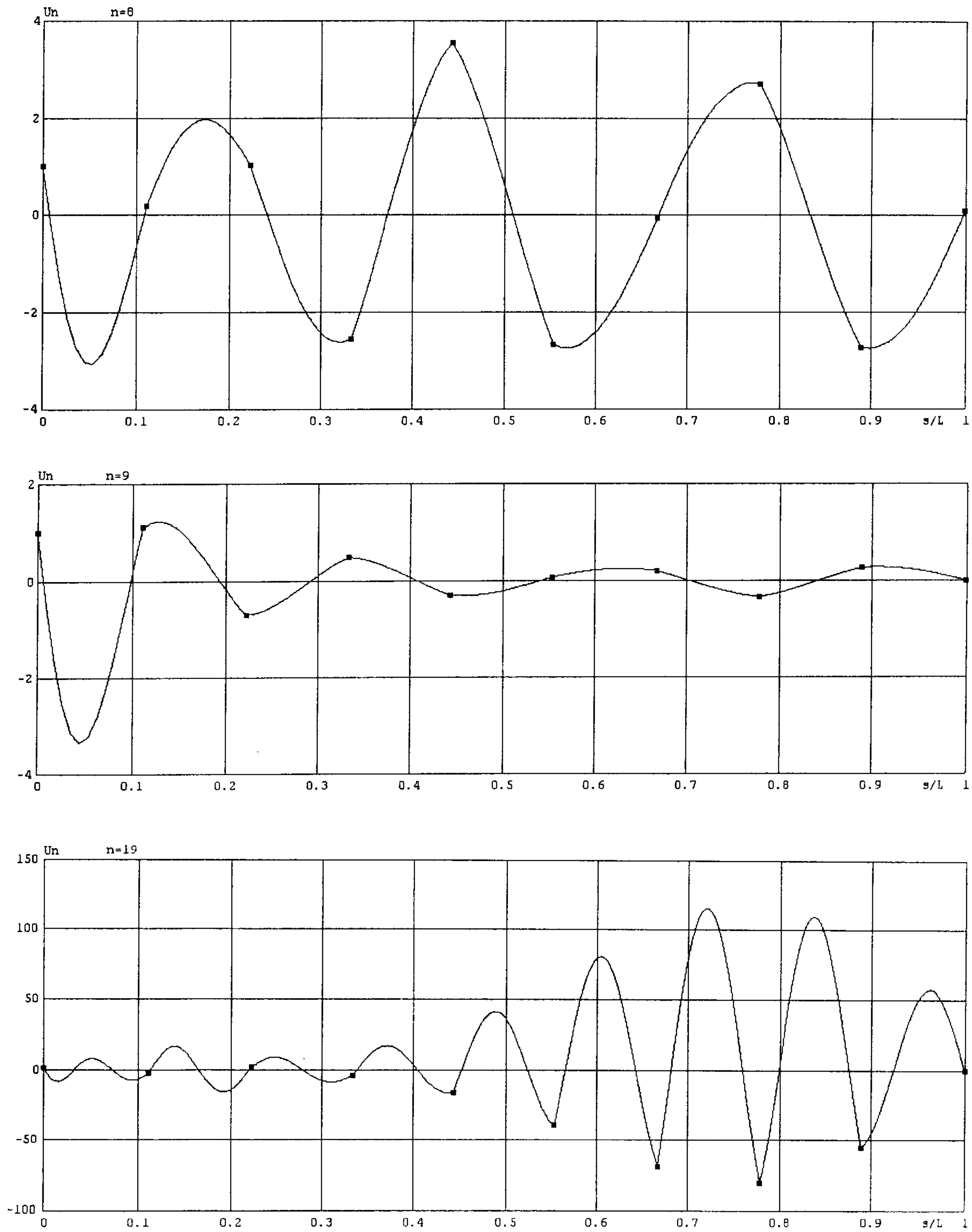

Fig. 5. Higher eigenforms of a spinning tether system ($n = 8, 9, 19$).

Also, the following relation for the eigenvalues can be derived from (22)

$$\beta_n^2 = \frac{1}{||U_n||} \int_A^B P\,(U_n')^2\, ds = 0. \tag{32}$$

Some eigenforms are shown in Fig. 4-5 for the same parameters as in case (b) of Fig. 3, namely, $L = 90$ km, $m_A = 250$ kg, $m_B = 11000$ kg, $m_k = 200$ kg, $k = 1, \ldots, 8$, connected with 10 km long uniform tethers of the following masses: 318, 365, 406, 438, 461, 473, 475, 473, 460 kg. The corresponding nontrivial eigenvalues ($n = 2, \ldots, 19$) are given below

$$\begin{array}{lll}
\beta_2 = 2.136, & \beta_8 = 10.497, & \beta_{14} = 20.182, \\
\beta_3 = 3.339, & \beta_9 = 11.355, & \beta_{15} = 20.573, \\
\beta_4 = 4.590, & \beta_{10} = 12.414, & \beta_{16} = 22.015, \\
\beta_5 = 5.912, & \beta_{11} = 15.549, & \beta_{17} = 23.714, \\
\beta_6 = 7.328, & \beta_{12} = 18.020, & \beta_{18} = 25.550, \\
\beta_7 = 8.853, & \beta_{13} = 19.320, & \beta_{19} = 27.529.
\end{array}$$

Generally, the n-th form has n nodes. Note that while the lower modes (Fig. 4) show smooth curves of average collective behavior, the higher modes (Fig. 5) exhibit a more peculiar interplay between the tether and embedded mass dynamics.

6. DECOMPOSITION OF MOTION

Using eigenforms obtained from the solution of the boundary problem (21) and the eigenvalue problem (22) for a simplified case of a stationary rotation, we can represent solutions of the general equations (3)–(4) in the form of a series expansion

$$\mathbf{R}(s,t) = \sum_{n=0}^{\infty} \mathbf{q}_n(t)\, U_n(s), \tag{33}$$

where the term $n = 0$ (trivial form $U_0 = 1$) represents, in essence, the orbital motion of the center of mass, $\mathbf{q}_0 = \mathbf{R}_C(t)$, and the term $n = 1$ (trivial form $U_1 = s - s_C$) describes a quasi-rigid rotation of an imaginary straight tether, $\mathbf{q}_1 = \boldsymbol{\tau}_1(t)$, where $\boldsymbol{\tau}_1$ is pointing along the imaginary straight tether line, so that

$$\mathbf{R}(s,t) = \mathbf{R}_C(t) + (s - s_C)\,\boldsymbol{\tau}_1(t) + \sum_{n=2}^{\infty} \mathbf{q}_n(t)\, U_n(s). \tag{34}$$

The higher order terms $n \geq 2$ represent tether oscillations about the imaginary straight line drawn through the center of mass C along vector $\boldsymbol{\tau}_1$. Kinematically, they do not contribute to the displacement of the center of mass and the quasi-rigid rotation because of the orthogonality conditions (26).

Note that the term with $\boldsymbol{\tau}_1$ also describes a uniform elongation of the tether system. If we disregard the higher order terms $n \geq 2$, then the tether elongation $\gamma = |\mathbf{R}'| = |\boldsymbol{\tau}_1| = \gamma_1$ will be the same for all tether elements.

Expression (33) yields similar kinematic and dynamic relations,

$$\dot{\mathbf{R}}(s,t) = \sum_{n=0}^{\infty} \dot{\mathbf{q}}_n(t)\, U_n(s), \qquad \ddot{\mathbf{R}}(s,t) = \sum_{n=0}^{\infty} \ddot{\mathbf{q}}_n(t)\, U_n(s), \tag{35}$$

or in terms of (34),

$$\begin{aligned}
\dot{\mathbf{R}}(s,t) &= \dot{\mathbf{R}}_C(t) + (s - s_C)\, \dot{\boldsymbol{\tau}}_1(t) + \sum_{n=2}^{\infty} \dot{\mathbf{q}}_n(t)\, U_n(s), \\
\ddot{\mathbf{R}}(s,t) &= \ddot{\mathbf{R}}_C(t) + (s - s_C)\, \ddot{\boldsymbol{\tau}}_1(t) + \sum_{n=2}^{\infty} \ddot{\mathbf{q}}_n(t)\, U_n(s),
\end{aligned} \tag{36}$$

where the derivatives are calculated with respect to the non-rotating geocentric frame $OXYZ$.

We can now substitute the second equation of (35) into the general equations (3)–(4), multiply by U_n, $n = 0, 1, 2, \ldots$, and sum over all tether elements and point masses. Applying the orthogonality conditions (26), we find that

$$\ddot{\mathbf{q}}_n = \frac{1}{||U_n||}\, (\mathbf{Q}_n + \mathbf{G}_n + \boldsymbol{\Phi}_n), \qquad n = 0, 1, 2, \ldots, \tag{37}$$

where $\mathbf{Q}_n$ is reduced to an integral of tension,

$$\begin{aligned}
\mathbf{Q}_n &= \mathbf{T}_A U_{nA} - \mathbf{T}_B U_{nB} + \sum_k (\mathbf{T}_{k+} - \mathbf{T}_{k-})\, U_{nk} + \int_A^B \mathbf{T}' U_n\, ds \\
&= -\int_A^B \mathbf{T}\, U_n'\, ds,
\end{aligned} \tag{38}$$

$\mathbf{G}_n$ is expressed through the inner product (27),

$$\begin{aligned}
\mathbf{G}_n &= \langle \mathbf{g},\, U_n \rangle \\
&= m_A (\mathbf{g}\, U_n)_A + m_B (\mathbf{g}\, U_n)_B + \sum_k m_k (\mathbf{g}\, U_n)_k + \int_A^B \rho\, (\mathbf{g}\, U_n)\, ds,
\end{aligned} \tag{39}$$

and $\mathbf{\Phi}_n$ is a generalized sum of non-gravitational forces,

$$\mathbf{\Phi}_n = \mathbf{F}_A U_{nA} + \mathbf{F}_B U_{nB} + \sum_k \mathbf{F}_k \, U_{nk} + \int_A^B \mathbf{F} \, U_n \, ds. \tag{40}$$

The system of ordinary differential equations (37) is equivalent to the original system of mixed partial and ordinary differential equations (3)–(4), because it is derived through the general transformation of variables (33) without any simplifying assumptions.

Using notations (34), and taking into account that $||U_0|| = M$ and $\mathbf{Q}_0$ vanishes because $U_0' = 0$, the motion of the center of mass is described by

$$\ddot{\mathbf{R}}_C = \frac{1}{M} \, (\mathbf{G}_0 + \mathbf{\Phi}_0). \tag{41}$$

Taking into account that $||U_1|| = J_C$ and $U_1' = 1$, the quasi-rigid rotation and uniform elongation are described by

$$\ddot{\boldsymbol{\tau}}_1 = \frac{1}{J_C} \, (\mathbf{Q}_1 + \mathbf{G}_1 + \mathbf{\Phi}_1), \qquad \mathbf{Q}_1 = -\int_A^B \mathbf{T} \, ds. \tag{42}$$

According to (34), the tangent to the tether line is defined as

$$\mathbf{R}' = \boldsymbol{\tau}_1 + \Delta\boldsymbol{\tau}, \qquad \Delta\boldsymbol{\tau} = \sum_{n=2}^{\infty} \mathbf{q}_n U_n'. \tag{43}$$

Assuming that $|\Delta\boldsymbol{\tau}| \ll |\boldsymbol{\tau}_1|$, the elongation can be approximated as

$$\gamma = |\mathbf{R}'| = \sqrt{|\boldsymbol{\tau}_1|^2 + 2(\boldsymbol{\tau}_1 \, , \Delta\boldsymbol{\tau}) + |\Delta\boldsymbol{\tau}|^2} \approx \gamma_1 + (\mathbf{e}_1 \, , \Delta\boldsymbol{\tau}) = \gamma_1 + \sum_{n=2}^{\infty} q_{en} \, U_n', \tag{44}$$

where

$$\gamma_1 = |\boldsymbol{\tau}_1|, \qquad \mathbf{e}_1 = \frac{\boldsymbol{\tau}_1}{\gamma_1}, \qquad q_{en} = (\mathbf{e}_1 \, , \mathbf{q}_n). \tag{45}$$

The tether tension depends not only on the elongation, but also on temperature, internal friction, creep history, and other factors. The following expression can be adopted within a certain range of conditions,

$$T = T_0 + E \, (\gamma - \gamma_*) + D \, \dot{\gamma}, \tag{46}$$

where T_0 is a reference tension, E is the tether longitudinal stiffness, D is the damping coefficient,

$$\gamma_* = \gamma_0 + \varepsilon \, (t - t_0) + \alpha \, (\Theta - \Theta_0), \tag{47}$$

γ_0 is the elongation under the reference tension T_0 at time t_0 and a reference temperature Θ_0, ε is the creep rate, α is the thermal expansion coefficient, and Θ is the current temperature of the tether element. Other terms can be added as needed.

Substituting (44) into (46), we derive

$$T = T_1 + \sum_{n=2}^{\infty}(E\, q_{en} + D\, \dot{q}_{en})\, U_n', \qquad T_1 = T_0 + E\,(\gamma_1 - \gamma_*) + D\,\dot{\gamma}_1, \tag{48}$$

and then calculate

$$\frac{T}{\gamma} \approx \frac{T_1}{\gamma_1} + \frac{1}{\gamma_1} \sum_{n=2}^{\infty} \left[\left(E - \frac{T_1}{\gamma_1}\right) q_{en} + D\, \dot{q}_{en}\right] U_n'. \tag{49}$$

Retaining only linear terms in $\mathbf{q}_n$, the integral of tension $\mathbf{Q}_n$ can now be represented as

$$\begin{aligned} \mathbf{Q}_n &= -\int_A^B \frac{T}{\gamma}\, \mathbf{R}'\, U_n'\, ds = -\int_A^B \frac{T}{\gamma}\left(\boldsymbol{\tau}_1 + \sum_{k=2}^{\infty} \mathbf{q}_k\, U_k'\right) U_n'\, ds \\ &\approx -\int_A^B \left(T_1 \mathbf{e}_1 + \sum_{k=2}^{\infty} \mathbf{c}_k\, U_k'\right) U_n'\, ds, \end{aligned} \tag{50}$$

where $\mathbf{e}_1 = \boldsymbol{\tau}_1/\gamma_1$ is a unit vector along the imaginary straight tether line and

$$\mathbf{c}_n = E\, \mathbf{e}_1 q_{en} + D\, \mathbf{e}_1 \dot{q}_{en} + \frac{T_1}{\gamma_1}\,(\mathbf{q}_n - \mathbf{e}_1 q_{en}), \qquad q_{en} = (\mathbf{e}_1,\, \mathbf{q}_n). \tag{51}$$

Expression (50) can be significantly simplified in the ideal case of a perfectly tapered tether. Let us define the tether reference state $T_0(s)$ as a stationary rotation at an angular rate Ω_0 free of external torques, as described in Section 4, with the exception that the tether is now elastic. Let us assume that the tether is perfectly tapered so that all tether elements have the same elongation γ_0 under the stationary tension T_0 at a given temperature Θ_0. Then, similarly to (11), the equilibrium tension profile can be determined from the boundary problem

$$\begin{aligned} T' &= -\rho\, \Omega^2 (s - s_C)\, \gamma_0, \\ T_A &= -m_A \Omega^2 (s_A - s_C)\, \gamma_0, \\ T_B &= m_B \Omega^2 (s_B - s_C)\, \gamma_0, \\ T_{k+} &= T_{k-} - m_k \Omega^2 (s_k - s_C)\, \gamma_0, \end{aligned} \tag{52}$$

and similarly to (20), the equilibrium tension can be expressed as

$$T_0(s) = \Omega_0^2 \gamma_0\, P(s), \tag{53}$$

where $P(s)$ is the solution of the boundary problem (21).

Within the linear elasticity region, the longitudinal stiffness of the tether can be related to its tension as

$$E(s) = \frac{T_0(s)}{\gamma_0 - 1} = k_E\, \Omega_0^2\, P(s), \qquad k_E = \frac{\gamma_0}{\gamma_0 - 1}. \tag{54}$$

With a strain on the order of $\gamma_0 - 1 \sim 0.01$, the coefficient $k_E \sim 100$.

The internal damping coefficient is usually considered directly proportional to the longitudinal stiffness and inversely proportional to the frequency of oscillations Ω_n, which gives

$$D(s, \Omega_n) = \frac{E(s)\,\eta}{\Omega_n} = \nu_n\, \Omega_0^2\, P(s), \qquad \nu_n = \frac{k_E \eta}{\Omega_n}, \tag{55}$$

where η is a loss factor, on the order of 0.1 for braided tethers.

After these substitutions, the first term under the integral in formula (50) takes the form

$$T_1 \mathbf{e}_1 = \Omega_0^2 P(s)\,[\gamma_0 + k_E\,(\gamma_1 - \gamma_*) + \nu_1\,\dot{\gamma}_1]\,\mathbf{e}_1 = \Omega_0^2 P(s)\, u_1\, \boldsymbol{\tau}_1,$$

where

$$u_1 = \frac{1}{\gamma_1}[\gamma_0 + k_E\,(\gamma_1 - \gamma_*) + \nu_1\,\dot{\gamma}_1], \tag{56}$$

and the expansion coefficients become

$$\mathbf{c}_n = \Omega_0^2 P(s)\, \left[k_E\, \mathbf{e}_1 q_{en} + \nu_n\, \mathbf{e}_1 \dot{q}_{en} + u_1\,(\mathbf{q}_n - \mathbf{e}_1 q_{en})\right].$$

If we assume that γ_* defined by (47) does not vary along the tether, *i.e.*, the creep rate, thermal expansion coefficient, and the temperature are the same for all tether elements, then we can apply the orthogonality condition (28) along with the eigenvalue relation (32) to derive

$$\mathbf{Q}_1 = -J_C\, \Omega_0^2\, u_1\, \boldsymbol{\tau}_1, \tag{57}$$

for $n = 1$ and

$$\mathbf{Q}_n = -||U_n||\, \beta_n^2 \Omega_0^2\, \left[k_E\, \mathbf{e}_1 q_{en} + \nu_n\, \mathbf{e}_1 \dot{q}_{en} + u_1\,(\mathbf{q}_n - \mathbf{e}_1 q_{en})\right] \tag{58}$$

for $n = 2, 3, \ldots$

Now, we can rewrite the equation of quasi-rigid rotation (42) as

$$\ddot{\boldsymbol{\tau}}_1 + \Omega_0^2\, u_1 \boldsymbol{\tau}_1 = \frac{1}{J_C}\,(\mathbf{G}_1 + \boldsymbol{\Phi}_1), \tag{59}$$

and the equations of tether oscillations (37), $n = 2, 3, \dots$, as

$$\ddot{\mathbf{q}}_n + \beta_n^2 \Omega_0^2 \left[k_E \, \mathbf{e}_1 q_{en} + \nu_n \, \mathbf{e}_1 \dot{q}_{en} + u_1 \left(\mathbf{q}_n - \mathbf{e}_1 q_{en} \right) \right] = \frac{1}{||U_n||} (\mathbf{G}_n + \mathbf{\Phi}_n). \qquad (60)$$

7. GRAVITATIONAL FORCES

The gravitational terms in the equations of motion (41), (59) and (60) are defined by (39). The variation of the main component of the gravitational acceleration $\mathbf{g}$ along the tether can be represented in the linear approximation in displacement from the center of mass as

$$\mathbf{g} = -\frac{\mu_E \mathbf{R}}{R^3} \approx -\frac{\mu_E \mathbf{R}_C}{R_C^3} + \frac{\mu_E}{R_C^3} \left[3\mathbf{e}_R \left(\mathbf{e}_R, \mathbf{r} \right) - \mathbf{r} \right], \qquad (61)$$

where μ_E is the gravity constant of the Earth, $\mathbf{e}_R = \mathbf{R}_C / R_C$ is a unit vector along the geocentric radius of the center of mass $\mathbf{R}_C$, and

$$\mathbf{r}(s,t) = (s - s_C) \, \boldsymbol{\tau}_1(t) + \sum_{n=2}^{\infty} \mathbf{q}_n(t) \, U_n(s) \qquad (62)$$

is the position vector relative to the center of mass.

Substituting expressions (61)–(62) into (39), and applying the orthogonality conditions (27) and the norm definition (29), we obtain

$$\begin{aligned} \mathbf{G}_0 &\approx -M \, \frac{\mu_E \mathbf{R}_C}{R_C^3}, \\ \mathbf{G}_1 &\approx J_C \, \frac{\mu_E}{R_C^3} \left[3\mathbf{e}_R \left(\mathbf{e}_R, \boldsymbol{\tau}_1 \right) - \boldsymbol{\tau}_1 \right], \\ \mathbf{G}_n &\approx ||U_n|| \, \frac{\mu_E}{R_C^3} \left[3\mathbf{e}_R \left(\mathbf{e}_R, \mathbf{q}_n \right) - \mathbf{q}_n \right], \quad n = 2, 3, \dots, \end{aligned} \qquad (63)$$

where M is the total mass of the system (30), and J_C is the moment of inertia of an imaginary system with an unstretched straight tether about the center of mass defined by (31).

Note that in the linear approximation, the higher modes of oscillations do not affect the motion of the center of mass and the quasi-rigid rotation about the center of mass, and there is no practical need to include higher order terms in $\mathbf{q}_n$ as long as typical amplitudes of tether oscillations in a momentum exchange system are relatively small. However, to achieve the required precision, it is necessary to include higher order terms in $(s - s_C) \, \boldsymbol{\tau}_1$.

The variation of the main (Newtonian) term of the gravitational acceleration along the line $(s - s_C)\,\boldsymbol{\tau}_1$ drawn through the center of mass is given by

$$\mathbf{g} = -\frac{\mu_E \mathbf{R}}{R^3} = -\frac{\mu_E\,[\mathbf{R}_C + (s - s_C)\,\boldsymbol{\tau}_1]}{|\mathbf{R}_C + (s - s_C)\,\boldsymbol{\tau}_1|^3} = -\frac{\mu_E}{R_C^2}\,\frac{\mathbf{e}_R + \varepsilon\mathbf{e}_1}{(1 - 2x\varepsilon + \varepsilon^2)^{3/2}} \tag{64}$$

where

$$x = -(\mathbf{e}_R, \mathbf{e}_1), \qquad \mathbf{e}_1 = \frac{\boldsymbol{\tau}_1}{\gamma_1}, \qquad \varepsilon = \frac{(s - s_C)\,\gamma_1}{R_C}.$$

As known in the theory of Legendre functions,

$$\frac{1}{(1 - 2x\varepsilon + \varepsilon^2)^{1/2}} = \sum_{n=0}^{\infty} P_n(x)\,\varepsilon^n,$$

where $P_n(x)$ are Legendre polynomials. Differentiating this equation with respect to x and dividing by ε, we find that

$$\frac{1}{(1 - 2x\varepsilon + \varepsilon^2)^{3/2}} = \sum_{n=0}^{\infty} P'_{n+1}(x)\,\varepsilon^n,$$

where P'_n are the first derivatives of the Legendre polynomials.

After substituting this expression in (64), we obtain

$$\mathbf{g} = -\frac{\mu_E}{R_C^2} \sum_{n=0}^{\infty} \left[\mathbf{e}_R\,P'_{n+1}(x) + \mathbf{e}_1\,P'_n(x)\right] \left[\frac{(s - s_C)\,\gamma_1}{R_C}\right]^n. \tag{65}$$

This series expansion converges rapidly because $(s - s_C)/R_C$ is typically small, on the order of 0.01. To determine a minimum number of terms required for practical computation, consider a simple inequality

$$n\left(\frac{L}{R_C}\right)^n \lesssim \delta, \qquad \text{or} \qquad n \gtrsim \frac{\ln(n/\delta)}{\ln(R_C/L)}, \tag{66}$$

where the left part estimates the contribution of the n-th term, L is the total tether length, and δ is a maximum acceptable relative error. Generally, all terms $n \geqslant N$, where N is the minimum number satisfying (66), can be dropped. For a typical momentum exchange system, it is sufficient to retain only 5 terms at the perigee, and 4 terms at the apogee to achieve 10-digit precision ($\delta \sim 10^{-10}$).

Expansion (65) can be also presented as

$$\mathbf{g} = \sum_{n=0}^{\infty} \mathbf{g}_C^n\,(s - s_C)^n, \qquad \mathbf{g}_C^n = \frac{1}{n!}\,\frac{\partial^n \mathbf{g}}{\partial s^n}\bigg|_C, \tag{67}$$

where the derivatives with respect to s are calculated along the line $(s - s_C)\tau_1$ drawn through the center of mass. For the Newtonian term, according to (65),

$$\mathbf{g}_C^n = -\frac{\mu_E \gamma_1^n}{R_C^{2+n}} \left[\mathbf{e}_R P'_{n+1}(x) + \mathbf{e}_1 P'_n(x)\right] \tag{68}$$

Note that expansion (67) can be treated more broadly to include all terms of the standard representation of the Earth gravitational field, as well as the gravitational fields of other celestial bodies.

Using (67), the generalized gravitational forces $\mathbf{G}_n$ (39) can be represented as

$$\mathbf{G}_n = \sum_{k=0}^{\infty} \mathbf{g}_C^k I_n^k, \qquad I_n^k = \langle (s - s_C)^k, U_n \rangle. \tag{69}$$

Applying the orthogonality conditions (27), norm definition (29), and trivial form properties (24)–(25), (30)–(31), we find that

$$\begin{array}{llllll} I_0^0 = M, & I_0^1 = 0, & I_0^2 = J_C, & \ldots & I_0^k = I_k, & \ldots \\ I_1^0 = 0, & I_1^1 = J_C, & I_0^2 = I_3, & \ldots & I_1^k = I_{k+1}, & \ldots \end{array} \tag{70}$$

where I_n are the high order moments,

$$I_n = m_A (s_A - s_C)^n + m_B (s_B - s_C)^n + \sum_k m_k (s_k - s_C)^n + \int_A^B \rho (s - s_C)^n ds. \tag{71}$$

We note also that

$$I_n^0 = I_n^1 = 0, \qquad n = 2, 3, \ldots \tag{72}$$

The practical benefit of using expansion (69) is that the quantities I_n^k can be precomputed to avoid integration of the gravitational force along the tether on each step of solution propagation.

Another practical question is to estimate how many terms of the gravitational field expansion (5) must be retained to achieve the required accuracy. The problem is in the slow convergence of the series expansion at low altitudes when the ratio R_E/R is close to 1.

On average, according to the Kaula rule [7], the normalized geopotential coefficients $\bar{C}_{nm}$ and $\bar{S}_{nm}$ decrease in inverse proportion to the second power of their degree,

$$\bar{C}_{nm}, \bar{S}_{nm} \sim \frac{10^{-5}}{n^2}. \tag{73}$$

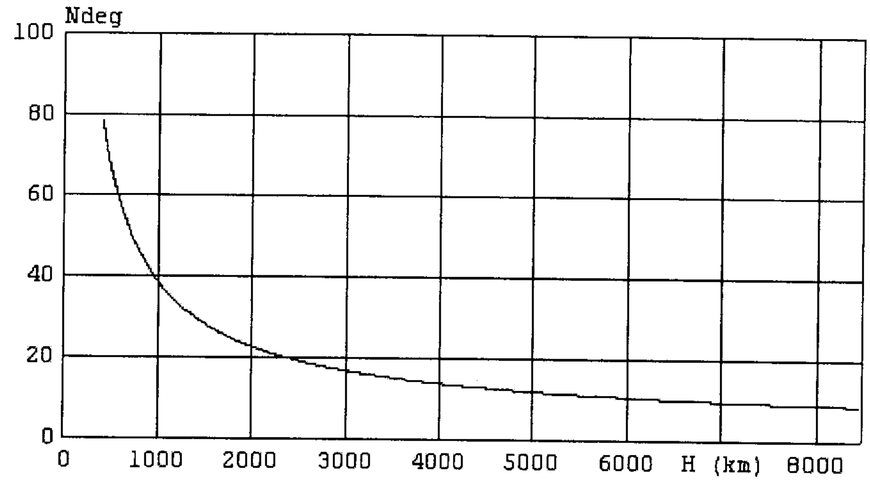

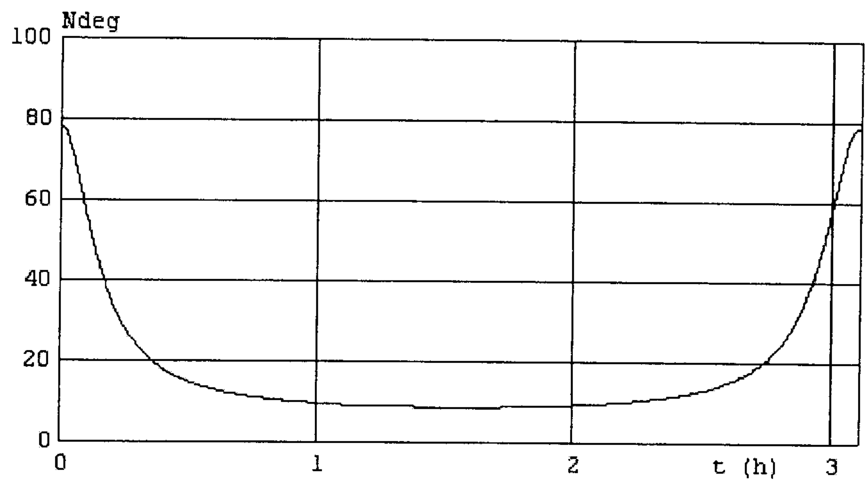

Fig. 6. Minimum degree of the geopotential expansion for MXER.

Taking this empirical rule into account, the following inequality roughly estimates the contribution of the higher degree terms to the acceleration of the center of mass of a momentum exchange tether system,

$$\frac{10^{-5}}{n}\left(\frac{R_E}{R_C}\right)^n \lesssim \delta, \qquad \text{or} \qquad n \gtrsim \frac{\ln(n\,\delta\cdot 10^5)}{\ln(R_C/R_E)}. \tag{74}$$

Numerical experiments show that a value of $\delta \sim 10^{-9}$ can be assumed for MXER to achieve better than 1 m prediction accuracy over one orbit. The minimum degree N that satisfies (74) is shown in Fig. 6 as a function of the geocentric radius and flight time. We see that a lower degree model is adequate for the most part of the orbit, but a model of a much higher degree is needed during perigee passages.

8. SIMULATION APPROACH

Now, we can gather all equations, and apply formulas for the gravitational forces derived in the previous section. The equation of motion of the center of mass (41) takes the form

$$\ddot{\mathbf{R}}_C = \mathbf{g}_C^0 + \frac{1}{M} \sum_{k=2}^{\infty} \mathbf{g}_C^k \, I_0^k + \frac{\mathbf{\Phi}_0}{M}, \tag{75}$$

the equation of the quasi-rigid rotation (59) can be rewritten as

$$\ddot{\boldsymbol{\tau}}_1 + \Omega_0^2 \, u_1 \boldsymbol{\tau}_1 = \mathbf{g}_C^1 + \frac{1}{J_C} \sum_{k=2}^{\infty} \mathbf{g}_C^k \, I_1^k + \frac{\mathbf{\Phi}_1}{J_C}, \tag{76}$$

and the equations of tether oscillation (37), $n = 2, 3, \ldots$, can be reduced to

$$\begin{aligned} \ddot{\mathbf{q}}_n + \beta_n^2 \Omega_0^2 \left[k_E \, \mathbf{e}_1 q_{en} + \nu_n \, \mathbf{e}_1 \dot{q}_{en} + u_1 \left(\mathbf{q}_n - \mathbf{e}_1 q_{en} \right) \right] = \\ \frac{\mu_E}{R_C^3} \left[3\mathbf{e}_R \left(\mathbf{e}_R, \mathbf{q}_n \right) - \mathbf{q}_n \right] + \frac{1}{||U_n||} \sum_{k=2}^{\infty} \mathbf{g}_C^k \, I_n^k + \frac{\mathbf{\Phi}_n}{||U_n||}. \end{aligned} \tag{77}$$

As noted earlier, very few terms $\mathbf{g}_C^k$ are needed to achieve the desired precision, and quantities I_n^k can be precomputed.

Equations (75)–(77) cleanly separate three dynamically different kinds of motions of the momentum exchange tether system. They are compact and flexible in sense that the number of the gravitational terms and the number of the tether oscillation modes can be selected depending on the desired accuracy. This opens a way to building a very computationally effective simulator.

Preliminary testing for a typical momentum exchange system showed that equations (75)–(77) can be integrated with a time step of about 4 seconds of orbital time, and it takes only a few seconds on a standard issue PC to propagate a solution over one orbit with 9–10 digit precision. More studies are needed to understand possible limitations of this approach.

REFERENCES

1. Moravec, H., A Non-Synchronous Orbital Skyhook, *Journal of the Astronautical Sciences,* **25(4),** Oct-Dec 1977, pp. 307-322.
2. Hoyt, R., Uphoff, C., Cislunar Tether Transport System, AIAA 99-2690, 1999
3. Hoyt, R., Design and Simulation of a Tether Boost Facility for The HASTOL Architecture, AIAA Paper 2000-3615, 36th Joint Propulsion Conference, July 2000.
4. Sorensen, K.F., Conceptual Design and Analysis of an MXER Tether Boost Station, AIAA 2001-3915, 2001
5. Beletsky, V.V. and Levin, E.M. Dynamics of Space Tether Systems. *Advances in the Astronautical Sciences,* AAS, **83,** 1993, Univelt, Inc.
6. Lemoine, F.G., Kenyon, S.C., Factor, J.K., Trimmer, R.G., Pavlis, N.K., Chinn, D.S., Cox, C.M., Klosko, S.M., Luthcke, S.B., Torrence, M.H., Wang, Y.M., Williamson, R.G., Pavlis, E.C., Rapp, R.H. and Olson, T.R. The Development of the Joint NASA GSFC and NIMA Geopotential Model EGM96, NASA Goddard Space Flight Center, NASA TP-1998-206891, July 1998.
7. Montenbruck, O. and Gill, E. *Satellite Orbits: Models, Methods and Applications,* Springer Verlag, 2000.